Modeling of Substrate Plate Preheating to Predict Efficiency in the Electron Beam Melting Process

M. Michatz[1,2]*, S. Janson[3], G. Schlick[2], I. Kuehne[4], A. Frey[1]
[1]University of Applied Sciences, Augsburg, BY, Germany
[2]Fraunhofer IGCV Research Institution, Augsburg, BY, Germany
[3]iwb Application Center Augsburg, BY, Germany
[4]Heilbronn University of Applied Sciences, Kuenzelsau, BW, Germany
*Corresponding author: marco.michatz@hs-augsburg.de

Abstract – The success of the production of metallic components via Additive Manufacturing depends largely on the process parameters. To ensure a stable process in Electron Beam Melting the range of the temperature at the point of beam impact on the upper side of the substrate plate requires a high degree of accuracy. However, the direct measurement of this temperature in the focus plane is not trivial due to the process conditions. This paper presents a model-based approach that supports the determination of this parameter. COMSOL Multiphysics® is utilized for replicating the preheating process. The data sets obtained from the simulation are compared to results from an experimental test setup to extract a specific loss factor for the preheating cycle. This factor adjusts the output power responsible for the generation of the critical focus temperature during the preheating cycle.

Keywords: Electron Beam Melting, EBM, Additive Manufacturing, AM, efficiency factor, substrate plate preheating, FEM

1. Introduction

Additive Manufacturing (AM) is revolutionizing the industrial sector for complex and individualized metallic components. The VDI 3404 guideline and the DIN EN ISO 17296 standard provide an overview of the technology and define the different AM procedures. They are essentially tool-free production processes with a high degree of design freedom. The most limiting factor of the widely established laser beam melting technology is the scan velocity due to the inertia of the mirrors [1]. In the Electron Beam Melting (EBM) process, this aspect is not relevant because electromagnetic coils deflect the beam to the desired position on the focus plane (see Fig. 3). The technology offers the potential to increase AM process capabilities by means of the following advantages [2]:

- Higher deflection speeds.
- The possibility to scan and heat several areas quasi-simultaneously.

Among these advantages, a transient physical effect is created primarily by the electrostatic charge between the powder particles, which leads to a sudden spread of the unsolidified powder (powder dislocation) in the vacuum chamber and thus impedes the build process [2, 3]. In order to counteract this phenomenon, a recurring preheating process is implemented in the build process. This intermediate step improves the adhesion of the powder to the substrate plate and the emerging material layers due to the subtle sintering processes that occur. During the building and preheating cycles, the energy transfer of the beam electrons to the impact area (focus plane) causes a complex and variable loss. The fundamental share of this loss is a consequence of backscattering and the emitted radiation by the deceleration of the electrons on the focus plane [2]. The unavoidable decimation of the initial power output prevents the simple calculation of the desired energy density and thus the beam focus temperature (T_{BF}) for the build process. The main reasons for the necessity of the reliable determination of T_{BF} are:

- To achieve the optimal process temperature to improve component quality and avoid process errors.
- Improving the powder adhesion effect of the preheating cycle by the occurrence of subtle sintering processes between the powder and the solid material.
- Effective minimization of residual stresses and component warpage by reducing the temperature gradient via the preheating cycle.

The direct measurement of T_{BF} would allow for immediate control of the output power via the EBM electronics,

but this measurement is considered difficult due to process conditions such as the prevailing high vacuum, the X-ray emission, etc. In the test-setup used, a thermocouple on the bottom side of the substrate plate determines a temperature close to T_{BF} to enable an experience-based adjustment of the output power for the generation of T_{BF}. When the build job progresses and the plate is lowered, precise adjustments become impossible. The knowledge of specific loss coefficients depending on the build progress would lead to a more reliable modification of the output power and could support the operation in the required temperature range of T_{BF}.

2. Fundamentals of Electron Beam Melting

The EBM process is a powder bed fusion process for the production of metallic components by local solidification of powder particles using an electron beam. Prior to this process, the 3D model of the component, including support structures, is first divided (sliced) into 2D layers containing all the information required for the selective melting (scanning) by the energy source. The fusion is achieved solely with the energy of the accelerated electrons impacting the unsolidified powder. The individual components and areas of the system used are shown schematically in Fig. 1. The beam generation, forming and guiding takes place in the beam generator whereas the powder application of the substrate plate through the recoating unit and the actual build process takes place separately in the vacuum chamber. To generate the beam, an accumulation of electrons (electron cloud) is generated in the electron source consisting of the cathode, a Wehnelt cylinder and anode by preheating the cathode. The electrons are then accelerated by a potential difference along the *Z*-axis.

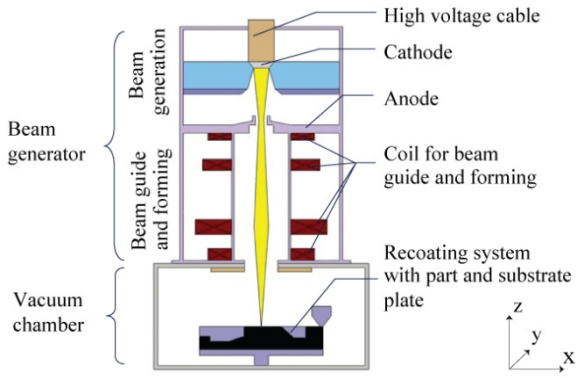

Figure 1. Schematic representation of the Electron Beam Melting system used [3].

The electron beam is focused by an electromagnetic lens system and deflected by coils according to the scan image [4]. Before each scanning cycle, the coating system applies an adjustable, thin powder layer of the substrate in the *XY*-plane (focus plane). In each individual layer, any position can be targeted in the focus plane, yielding a considerable design freedom. The successive lowering of the substrate plate in discrete steps in the *Z*-direction defines the resolution of the component or the layer thickness [5]. The EBM process cycles are performed under constant vacuum. This atmosphere is mainly required for the operation of the electron beam. The continuous vacuum also allows the processing of highly reactive materials and provides a high degree of thermal insulation [4].

2.1. Process deficiencies

Besides the previously mentioned uncontrolled powder dislocation in the vacuum chamber, other deficiencies exist which can prevent the completion of the build-job. In Laser Beam Melting, residual stresses are induced by thermal loads as a result of the local melting in the beam impact area [6]. This aspect may also apply to the EBM technology in the case of insufficient preheating. The formation of a large temperature gradient between the scanned area and the boundary zone can be assumed as the reason for the residual stresses due to the rapid heating and the low thermal conductivity of the surrounding substrate. A high gradient also leads to cracks in the microstructure and can cause delamination (see Fig. 2) and general component deformation. This weakens the load-bearing capacity of the component [7]. The aforementioned preheating process, between the coating and scanning cycles, not only improves powder adhesion but also leads to a reduction of this temperature gradient between the molten substrate and the unexposed areas. At the same time, the material shows a tendency to plastic flow. Both effects significantly reduce the internal stresses in the component and their negative effects [6]. Another shortcoming is the formation of melt agglomerates, as shown in Fig. 2, by unstable and inconsistent melt baths which can also lead to the termination of the whole build process [1].

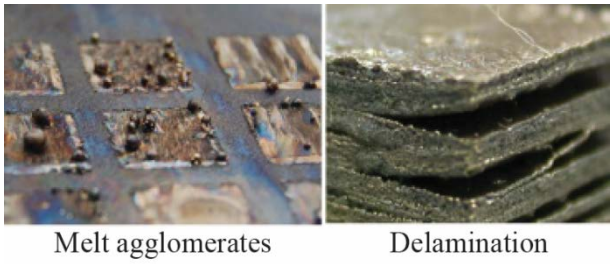

Figure 2: Process deficiencies (*left* melt agglomerates, *right* delamination) [1].

2.2. Process parameters

As shown above, maintaining a certain temperature range during the scanning and preheating cycles is a decisive factor for the successful build-up. Since the electron beam is utilized for both applications, the area energy E_{area} serves as the main parameter. This variable energy is formed mainly by the applied scan strategy and the EBM output power P_{out} as shown in Eq. (3). Within the scope of this work, E_{area} is adjusted solely by the output power P_{out} via the beam current I_{beam} in the EBM electronics since the scan-strategy and voltage remains constant. During the power input by the electron beam, unavoidable complex losses occur. These losses are simplified in this work, in the form of an efficiency factor η_{eff} as described in Eq. (4). The factor can be found for different characteristic scan-scenarios to improve the reproducibility of the temperature range of T_{BF} by simply considering the corresponding factor when setting the system parameters.

3. Use of COMSOL Multiphysics®

The simulation of the preheating process is performed in COMSOL Multiphysics® by a transient study of a 3D model using the Heat Transfer in Solids module. The model represents a simplified description of the complex physical effects in the EBM process. However, the overall efficiency factor can be derived with sufficient accuracy by comparison to an experimental test setup. In the model, the EBM output power acts as a boundary heat source on the substrate plate surface. To simulate the temperature of the thermocouple for the subsequent comparison, a measurement point is created and evaluated at the identical location. A type K thermocouple is used on the bottom side in the center of the substrate plate (see Fig. 3). Since the general EBM process is in a high vacuum state during each cycle, the natural convection of the model is neglected.

3.1. Modeling and parameters

The substrate plate (Fig. 3) consisting of mild steel (1.0144) is imported directly into COMSOL Multiphysics® as a 3D geometry object based on the CAD model of the design via the CAD Import Module. For reasons of simplicity, the complete vacuum chamber and the device for lowering the substrate plate are left out of the modeling process. The marked area A_{heat} in Fig. 3 shows the beam impact area of the preheating cycle. This surface has a machined surface characteristic compared to the remaining bare or oxidized surfaces.

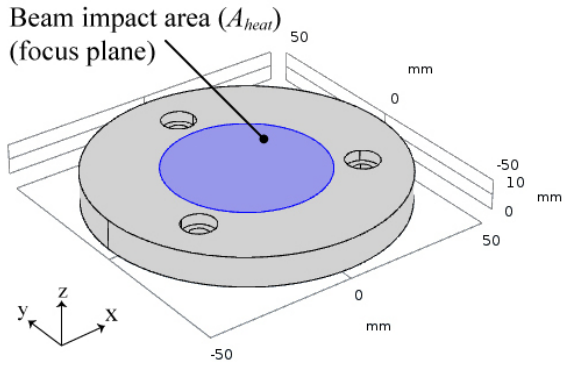

Figure 3. Substrate plate with the beam impact area A_{heat} for preheating

These different surface finishes are mapped by corresponding values of the emissivity ε depending on the prevailing temperature according to [8]. Diffuse Surface boundary conditions are applied to address cooling in different plate regions.

3.2. Mesh

A User-controlled mesh is set up. Mesh independence of the solution is investigated by a mesh refinement study. The resolution of the mesh is refined particularly in the area of the electron beam impact (cf. Fig. 4 version A). Also, the mesh distribution in the direction of the electron beam *(Z*-direction) is investigated. The resulting values are checked at several points for their differences. Due to the negligible deviation of the results, it is assumed that the mesh version B in Fig. 4 is sufficient within the scope of the measurement accuracy and is therefore used for the simulations.

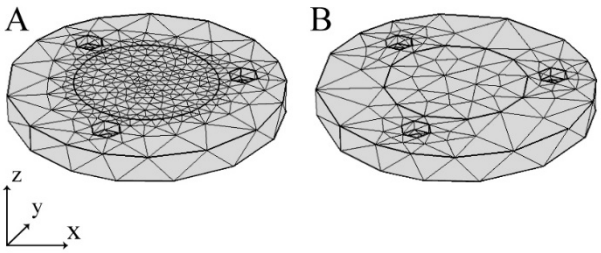

Figure 4. User-controlled mesh

3.3. Modeling of the beam power input

The local exposure by the beam with the most basic scan strategy can be understood as a repetitive - horizontal traversing - alongside a line through the punctual beam focus. The procedure is roughly comparable with the general principle of a cathode ray tube television. Since this process is high frequency during the preheating and selective scanning cycles by the electron beam the heat

flow of the substrate plate is considered to be inertial. Therefore, the energy input can be modeled by the spatial- and time-dependent heat flux density q_0, as contained in the PDE describing the thermal behavior in the modeling domain:

$$\rho C_p \frac{\partial T}{\partial t} + \rho C_p u \cdot \nabla T + \nabla \cdot q_0 = Q + Q_{ted} \qquad (1)$$

$$\text{with: } q_0 = \frac{P_{out}}{A_{heat}} = -k\nabla T \qquad (2)$$

Where C_p is the specific heat capacity at constant pressure, ρ is the mass density of the material, Q is the heat source and Q_{ted} is the thermoelastic damping. The temperature $T = T(x, y, z, t)$ is a function of three Cartesian variables (x, y, z) and a time variable *t*. In the term of advection, u represents the velocity field. The conduction heat flux density per unit area through a surface, as q_0 in Eq. (2), is proportional to the negative temperature gradient across the surface, where k describes the thermal conductivity. In this work q_0 can be defined by the ratio between the output power P_{out} and the exposed area A_{heat}. Due to the constant scan-strategy and voltage U, the output power P_{out} is adjusted directly via the beam current I_{beam} as:

$$P_{out} = U \cdot I_{beam} \qquad (3)$$

In order to verify a homogeneous temperature distribution during the preheating cycle, the local distribution of P_{out} needs to be considered. For that purpose, a high-performance camera is used to record near-infrared (NIR) images, as shown in Fig. 5, to evaluate the heat distribution of the impact area during the preheating cycle. The procedure is part of the pre-process of the EBM component production in the experimental setup. Once successful, it may only be repeated after fundamental changes are made to the process parameters, the scan strategy or the substrate plate itself. The generated NIR image is converted to a gradient image by analyzing and inverting the qualitative distribution (Fig. 5) of the captured thermal radiation values. This converted gradient image (an example is shown in Fig. 6) is then applied in the EBM beam control application to reduce the centric heat accumulation. Within the gradient image - which acts as a preheating pattern - the black areas correspond to regions with little or no power input whereas the white areas lead to the maximum possible energy input. The process described above is repeated until there is no noticeable heat accumulation due to the iterative optimization of the local beam intensity. The final gradient image represents the scan template for the preheating cycle.

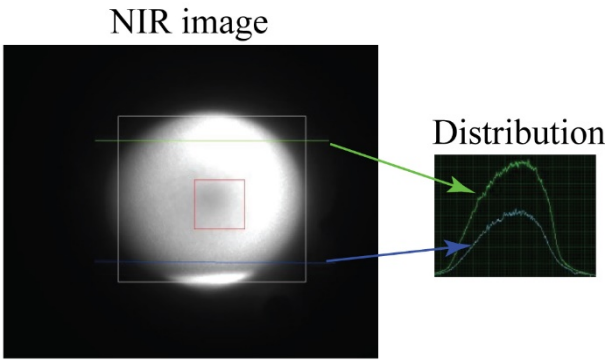

Figure 5. Near Infrared Image capturing (*left* NIR Image of A_{heat}, *right* distribution of thermal radiation)

To implement the gradient in the model, the template is mapped as a function *BI(x,y)* within the area A_{heat} via the COMSOL Image Function. The function modulates the Heat Flux settings by adjusting the Heat Rate in accordance with the percentage of the required heat load. This provides a realistic spatial distribution of the heat flow in the simulation. The application of this distribution function promises, in addition to uniform preheating, a heat cycle that is as efficient as possible with regard to beam-based heating.

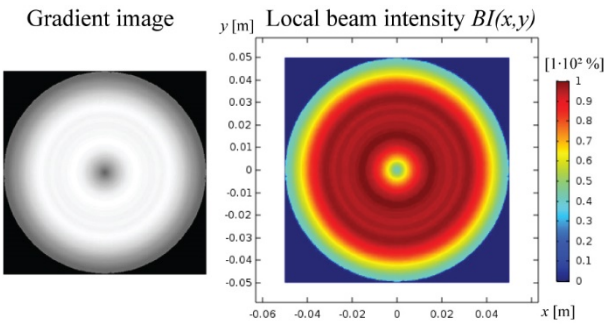

Figure 6. Image conversion to reduce heat accumulation in the preheating cycle (*left* final gradient image, *right* derived image function)

4. Experimental methodology

In order to determine the specific loss factor of the electron beam in the preheating cycle, the experimental data are compared to the simulation. In the experiment, the preheating is operated for 45 minutes at reduced power P_{real} (1100 W) to inhibit premature melting. Thereby the temperature value at the measuring point is recorded every 20 seconds. Under these operating conditions, the

system gradually approaches a state of equilibrium. Temperature changes are negligible after 45 minutes within the accuracy range of the used thermocouple. In a first simulation, the loss-free temperature value is found. Then, the modeled beam power is reduced with the aid of a Parametric Sweep until the simulated and the measured equilibrium temperature values coincide. The efficiency factor η_{eff} is then easily found by the ratio of the set input power P_{in} and the real output power P_{real}:

$$\eta_{eff} = \frac{P_{in}}{P_{real}} \tag{4}$$

4.1. Results

Fig. 7 shows the preheated substrate plate after a heating interval of 45 minutes. The beam impact area is located on the top and the position of the thermocouple is located on the bottom of the substrate plate. At the measurement point, a temperature of 840 °C is simulated for $P_{out} = 700$ W. This value in comparison to the actual power settings $P_{real} = 1100$ W results in an efficiency of $\eta_{eff} = 0.64$. This considerable efficiency loss can be explained by the interactions at the atomic level of the material.

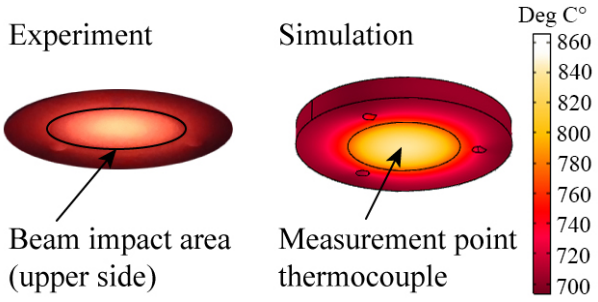

Figure 7. Substrate plate during the preheating cycle (*left* upper side from the experiment, *right* temperatures at the bottom side in the simulation)

The kinetic energy is largely converted into excitation energy. In the lattice structure of the material, the motion energy is increased until the material melts or evaporates. A large part of the loss is attributed to the emerging thermal radiation, the backscattering, the formation of secondary electrons and the process-related X-ray emission due to the deceleration of the electrons at the surface [2]. The calculated value has no general validity since the efficiency of an electron beam according to [1, 2] depends on factors such as geometry, material and temperature. The efficiency is in the expected range of 60 % for steel with a smooth surface to 90 % for the occurrence of a vapor capillary [2, 9].

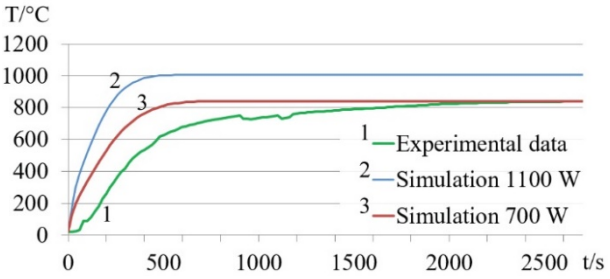

Figure 8. Adjustment of the output power to extract the efficiency factor

The adjustment of the EBM output power P_{out} can be seen in Fig. 8. Graph 1 represents the measurement during preheating in the test setup. The second graph shows the ideal power input without any loss while preheating the substrate plate. The third graph indicates the final parametric adjustment of the output power where the assumed equilibrium temperature values match.

5. Discussion and outlook

The extraction of the efficiency is based only on the adjustment of the equilibrium temperature. Nevertheless, in the following the transient behavior will be discussed in some detail.

First, there is a significant difference in the transient behavior between simulated an experimental data. In order to achieve fast computational times, some setup components are not included in the model. For example, the device that moves the substrate plate in the *Z*-direction and the entire machine bed. Compared to the experimental setup, the model has a significantly lower mass, which explains the more rapid temperature rise in the simulation. Therefore, to increase the model accuracy additional details should be taken into account. Furthermore, the emissivity is assumed to be constant in the model. For an improved modeling of the transient behavior, a temperate dependent emissivity should be applied. Second, the unsteadiness in the measurement data (first graph in Fig. 8) in the time range of 900 s – 1200 s results from a particular operation of the experimental setup. No effort is made here to incorporate these details into the model.

Finally, for calculating the efficiency factor during the additive build-up process, the model must be supplemented by the powder layer and a replica of a characteristic scanning pattern. This is due to the fact that the efficiency factor cannot be given as a general value and the building process deviates significantly from the simulated initial preheating cycle without a powder layer.

6. Summary

Among the innovative additive manufacturing processes, the EBM process has great potential to further increase the market share of AM technologies. By the application of a fast scanning electron beam for a layer by layer selective melting of metal powders, the productivity can be increased by melting different areas quasi-simultaneously.

The temperature in the focus area of the beam is crucial for the success of the build process. Knowledge of the complex losses of the electron beam in the form of loss factors in the various stages of different build scenarios can reduce the effort required to maintain the critical process temperature. This paper describes a model-based approach to extract the loss factor in the preheating cycle by replicating the preheating process by means of a simulation with the Finite Element Method. The simulated equilibrium temperature is calibrated through experimental data extracted at the bottom of the substrate plate. A loss coefficient of 0.64 for the preheating procedure for this experimental setup is found. This is in reasonable accordance with values given in [9]. The extracted value is applied to optimize the parameters of the electron beam of the system used to maintain the temperature window of the necessary preheating cycles. Since the value depends on geometry, material and temperature, the loss coefficient cannot be stated generally [1]. However, the simulation model offers a simple instrument for the tailored determination of further loss coefficients.

7. References

[1] M. F. Zäh & S. Lutzmann, Modelling and simulation of electron beam melting. *Production Engineering*, **Vol. 4**, pp. 15–23 (2010)

[2] M. Kahnert, *Scanstrategien zur verbesserten Prozessführung beim Elektronenstrahlschmelzen (EBM)*. Herbert Utz (2015).

[3] M. Kahnert, S. Lutzmann & M. F. Zäh, Layer formations in electron beam sintering. *Solid freeform fabrication symposium*, pp. 88–99 (2007)

[4] B. Klöden et al., Elektronenstrahlschmelzen - ein pulverbettbasiertes additives Fertigungsverfahren; In: *Entwerfen Entwickeln Erleben - Beiträge zur virtuellen Produktentwicklung und Konstruktionstechnik*, Stelzer, Ralph (Ed.). TUDpress (2016).

[5] A. Gebhardt, *Generative Fertigungsverfahren*: *Additive Manufacturing und 3D-Drucken für Prototyping - Tooling - Produktion*. München. Hanser (2016).

[6] D. Buchbinder et al., Untersuchung zur Reduzierung des Verzugs durch Vorwärmung bei der Herstellung von Aluminiumbauteilen mittels SLM. *RTejournal - Forum für Rapid Technologie*, **Vol. 8** (2011)

[7] C. Casavola, S. L. Campanelli & C. Pappalettere, Experimental analysis of residual stresses in the selective laser melting process. *Proccedings of the XIth International Congress and Exposition* (2008)

[8] J. R. Singham, Tables of emissivity of surfaces. *International Journal of Heat and Mass Transfer*, **Vol. 5**, 1-2, pp. 67–76 (1962)

[9] H. Schultz, *Electron beam welding*. Elsevier (1994).